Available online at www.sciencedirect.com
ScienceDirect
Physics Letters A 360 (2006) 84–91
PHYSICS LETTERS A
www.elsevier.com/locate/pla

Chaotic wave trains in an oscillatory/excitable medium

A. Rabinovitch [a,*], M. Gutman [a], Y. Biton [a], I. Aviram [b]

[a] *Physics Department, Ben-Gurion University of the Negev, Beer-Sheva 84105, Israel*
[b] *35, Shederot Yeelim, Beer-Sheva 84730, Israel*

Received 23 February 2006; received in revised form 11 July 2006; accepted 18 July 2006

Available online 4 August 2006

Communicated by C.R. Doering

Abstract

We study the chaotic dynamics of a heterogeneous reaction–diffusion medium composed of two uniform regions: one oscillatory, and the other excitable. It is shown that, by altering the diffusion coefficient, local chaotic oscillations can be induced at the interface between regions, which in turn, generate different chaotic sequences of pulses traveling in the excitable region. We analyze the properties of the local chaotic driver, as well as the diffusion-induced transitions. A procedure based on the abnormal frequency-locking phenomenon is proposed for controlling such sequences. Relevance of the obtained results to cardiac dynamics is briefly discussed.

PACS: 05.45.-a; 41.20.Jb

1. Introduction

Wave processes in excitable reaction–diffusion systems have been widely discussed recently. Besides the obvious theoretical interest, these studies allow deeper understanding of the complex dynamics of real periodically stimulated excitable media, a prominent example of which is the cardiac muscular tissue, the myocardium. This tissue supports the propagation of pulses of cardiac electrical activity in the form of action potentials generated by a self-oscillating pacemaker region, i.e., the sinus node (SN) [1,2]. Strongly chaotic sequences of action potential pulses are sometimes associated with serious cardiac dysfunctions (e.g., atrial or ventricular fibrillation, AF or VF), and various controlling techniques for their elimination have recently been proposed [3–6]. On the other hand, exactly periodic sequences of action potentials resulting in purely periodic heartbeats are also abnormal cardiac phenomena [7]. (A possible way to combat them by the use of different *anti*control strategies was suggested [8,9].) In order to achieve the ability to control this chaotic dynamics, it is important to clarify the conditions for generation of such wave trains. Some chaotic regimes were previously obtained in excitable systems by applying external periodic stimuli of different waveforms, amplitudes and frequencies [10–14]. However, diffusion coupled periodic sources leading to the generation of chaotic wave trains have rarely been discussed. For example, chaotic dynamics was obtained in chemical systems composed of a few coupled excitable and oscillatory cells [15,16]. Note that driving the excitable system by a coupled extended self oscillating (limit cycle, LC) region differs from an external forcing in that: (a) the driver waveform better simulates the natural pacer during steady operation; (b) considerable interplay takes place between the coupled regions, altering the ensuing dynamics, and (c) diffusion and size effects can be examined.

In the present work we investigate a heterogeneous reaction–diffusion medium composed of two adjacent uniform regions, one of which operates in an oscillatory regime, while the second is in an excitable mode. Such a simplified system allows us to generate chaotic wave trains traveling in the excitable region. It is shown that the regions' interface operates as a *local* chaotic driver, and is responsible for generation of chaotic wave trains. The simulations indicate that variation of the diffusion coefficient drastically changes the type of interface oscillations. As a result, different wave trains can propagate in the excitable re-

* Corresponding author.
E-mail address: avinoam@bgumail.bgu.ac.il (A. Rabinovitch).

0375-9601/$ – see front matter
doi:10.1016/j.physleta.2006.07.051

gion. This phenomenon is an interesting case of the so-called diffusion-induced chaos, which was a subject of several recent studies (see, e.g., [17,18]). It is also shown that the character of interface oscillations depends on the sizes of the two uniform regions. Namely, an increase in the size of the LC region is similar to an increase in the diffusion coefficient, whereas a size increase of the excitable region results in an opposite effect. In addition, the frequency of oscillations in the LC region also plays a role in the way these wave trains are generated. Thus, higher-frequency oscillations of practically equal amplitude generate even more chaotic wave trains. A procedure based on the abnormal frequency-locking phenomenon [19] is proposed for controlling such trains. In order to produce the desired effects, the parameter values of the model system were chosen in a range which turned out to be quite wide. Finally, the obtained results are invoked to portray chaotic-like cardiac pathologies, thus extending our models [19–21] of the cardiac pacemaker.

2. A diffusion induced local chaotic driver

The generation of chaotic wave trains is examined in a one-dimensional (1D) reaction–diffusion medium which is divided at a selected interface point x_0, into two uniform space regions of equal size. The left uniform region operates in an LC mode, while the right one is in an excitable regime. For this purpose we solve the FitzHugh–Nagumo (FHN) equations [22]:

$$\frac{\partial v}{\partial t} = D\frac{\partial^2 v}{\partial x^2} + v(v-a)(1-v) - w,$$
$$\frac{\partial w}{\partial t} = \varepsilon(v - dw), \tag{1}$$

where $a = a_1$, $\varepsilon = \varepsilon_1$, $d = d_1$ for $0 \leqslant x < x_0$, and $a = a_2$, $\varepsilon = \varepsilon_2$, $d = d_2$ for $x_0 \leqslant x \leqslant L$. Here $v(x,t)$ stands for an *activator*, embodying, e.g., the cardiac action potential, while $w(x,t)$ is an *inhibitor*, or a *refractoriness* function. D is the diffusion coefficient, a is the *excitability* parameter, and ε is a parameter, usually small, measuring the ratio between the time constants of the activator and the inhibitor; d is a parameter which, together with ε, determine the speed of growth of w. The time t is measured in units of the activator time constant. Neumann boundary conditions are imposed at both ends of the integration domain.

Let us recall (see, e.g., [23]) that a may be either positive or negative; if a is negative below a certain threshold value, the system will be in a limit-cycle regime, whereas positive values of a correspond to an excitable mode. We use the value $a_1 = -0.16$ throughout this work which puts the left region in an LC regime (one unstable fixed point at $v = w = 0$), and $a_2 = 0.015$, or $a_2 = 0.12$ in the excitable region to the right (one stable fixed point at $v = w = 0$). The diffusion coefficient D is the same for both regions of space, and $L = 200$. All parameters and variables are dimensionless.

The numerical integration of the system (1) was carried out using the unconditionally stable Crank–Nicolson method [24]. The values of time and space intervals, used in all numerical experiments, were $\Delta t = 0.5$ and $\Delta x = 1$. In order to avoid transient processes observed in the case of *locally* excited uniform LC regions [25,26], the initiating excitation here (amplitude ~ 0.8) was generally applied at $t = 0$ throughout the entire left region.

The numerical simulations results are presented in Fig. 1. As a consequence of the simultaneous initial excitation, and with the exception of a narrow transient zone near the interface, almost all points of the LC region exhibit monotonic bulk oscillations with zero phase lag. The intrinsic LC period is $T = 70$, and amplitude 0.76. (Fig. 1(a)). This extended periodic source, nevertheless, induces in the excitable region a sequence of pulses separated by chaotically varied time intervals (Fig. 1(b)). Such a chaotic wave train arises after period doubling bifurcations (Fig. 2), and represents an example of the so-called *phase* chaos, e.g., [27–29]. Here we show that such chaotic wave trains can be obtained in a wide range of excitable systems as a result of complex interactions with the adjacent LC region. The simulations also demonstrate that the variation of the diffusion coefficient D drastically changes the chaotic dynamics of the pulses traveling in the excitable region.

To clarify the underlying mechanism of the chaotic wave trains generation we propose a simplified explanation as follows: let us consider the local oscillations at the interface point x_0, (representing a thin layer of excitable points) shown in Fig. 1(c). These chaotic oscillations can only be induced by the diffusion current from the nearest LC points, since the point x_0 belongs to the right-hand excitable region. When the amplitudes of these induced oscillations exceed a certain threshold value, they initiate pulses traveling in the rest of the right-hand region. Since the time intervals between oscillations with sufficiently large amplitudes are chaotic, they result in chaotic sequences of traveling pulses. Thus the interface layer, of sufficient (liminal) width, see, e.g., [30], operates as a *local internal* driver whose complex dynamics is responsible for the generation of a chaotic wave train.

Since the local oscillatory dynamics at the interface arises as a result of diffusion coupling with the self-oscillating points, it can be transformed by changing the value of the diffusion coefficient D. Diffusion-induced bifurcation transitions between different types of interface oscillations are presented in Fig. 2. Starting from $D = 0$, it is evident that an increase in D, firstly leads to the appearance of very small oscillations (Fig. 2(a)), then goes through a cascade of period doubling bifurcations (Fig. 2(b), (c)), and further on, into chaotic oscillations with increasing, but still low amplitudes (Fig. 2(d)). An additional increase in D leads to the appearance of few spikes of significantly larger amplitudes, shown in Fig. 2(e). These large-amplitude intermittent spikes initiate traveling pulses in the right region.

To analyze these diffusion-induced bifurcations, let us consider the way in which the corresponding return maps change with D (Fig. 3). These maps represent successive maxima of v: M_{j+1} vs. M_j. Fig. 3(a) represents for $D = 1$ a chaotic map corresponding to the small-amplitude time series of Fig. 2(d), situated in a limited portion of the map plane, roughly $0.3 \leqslant M_j \leqslant 0.4$. With increasing D the attractor increases in size now spreading over the entire range $0 \leqslant M_j \leqslant 1$. Fig. 3(b) shows for

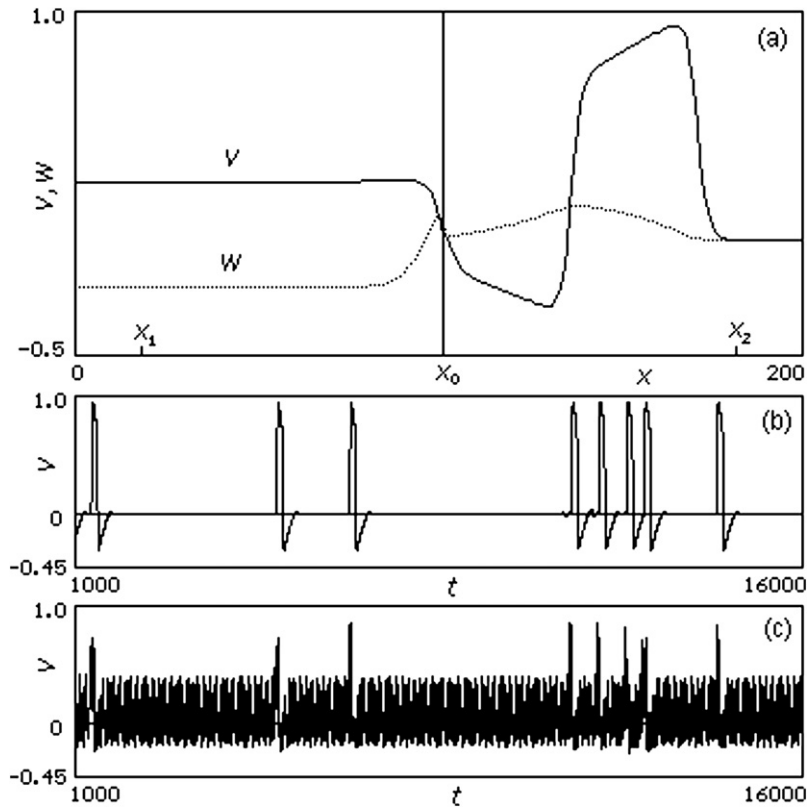

Fig. 1. The development of chaotic wave trains in a medium with two uniform regions: the LC region ($a_1 = -0.16$, $\varepsilon_1 = 0.06$, $d_1 = 1$, intrinsic period $T = 70$, $\Delta t = 0.5$) on the left, and the excitable region ($a_2 = 0.015$, $\varepsilon_2 = 0.005$, $d_2 = 3$) on the right; $D = 8$ throughout. (a) Synchronized bulk oscillations in the whole left region (except for a narrow transient zone near the interface) generate pulses propagating in the right region; (b) chaotic time series of pulses in the right region at the point x_2 ($x = 180$); (c) intermittency at the interface x_0 ($x = 100$) (see expanded time scale in Fig. 2(e)). There is a one-to-one correspondence between high amplitude pulses in frames (b) and (c), delayed indistinguishably at the figure scale. Remark: the snapshot in frame (a) is obtained at *any* time t corresponding to a high amplitude spike in frame (b).

$D = 8$ that, seemingly, two separate parts of the attractor coexist, between which the motion switches chaotically. The part of the map situated inside the little dotted frame approximately corresponds to the small amplitude oscillations as in Fig. 3(a), while the rest of the map corresponds to the large-amplitude intermittent spikes in Fig. 2(e). With further increase in D, the number of large-amplitude spikes increases significantly forming an almost closed chaotic contour (Fig. 3(c) for $D = 200$). Their chaotic behavior arises due to perturbation induced by the chaotic diffusion current Dv_{xx} from the adjacent LC region.

We wish to emphasize that, unlike the 1D maps obtained for periodically forced FHN excitable systems [12,14], all return maps of Fig. 3 portray the dynamics of a *chaotically* forced excitable system (the interface), and are therefore more complicated.

A very strong diffusion coupling, on the other hand, plays an inhibiting action on the generation of chaotic wave trains. More precisely, an increase in D from 480 to 600 results in bifurcation transitions from large-amplitude intermittent chaos to chaos of small amplitude, and then, via a set of inverse period-doubling bifurcations, to a complete disappearance of oscillations at the interface. Moreover, since a very strong diffusion current drastically decreases phase differences between adjacent excitable points, most of them (except a few points in a narrow transient zone) are compelled to oscillate in phase. These diffusion-induced synchronous oscillations prevent the propagation of pulses even though the interface by itself does exhibit large-amplitude spikes.

Returning to the small oscillations of Figs. 2(b), (c), the following question arises: why are they unable to generate propagating pulses in spite of being in considerable excess of the excitation threshold for an *uncoupled* interface point? The qualitative explanation is that strong diffusion causes a spread of the disturbance into the following excitable points, and can increase the threshold of interface excitation [31]. A very small diffusion coupling, on the other hand, also stops normal propagation of pulses. In this case the amplitudes of traveling pulses progressively decrease, and the pulses completely disappear after crossing some fixed space interval. This interval rapidly shrinks with further decrease of D.

One may conclude therefore that, in order to generate chaotic wave trains, the diffusion coupling must, on the one hand, be sufficiently large in order to induce oscillations with super-threshold amplitudes at the interface, and to support normal propagation of pulses in the excitable region. On the other hand, it must be small enough in order not to enlarge the threshold of the interface excitation too much, or to induce in-phase oscillations in nearly all excitable points.

Additional numerical experiments were performed in which external excitations were periodically applied at a single point

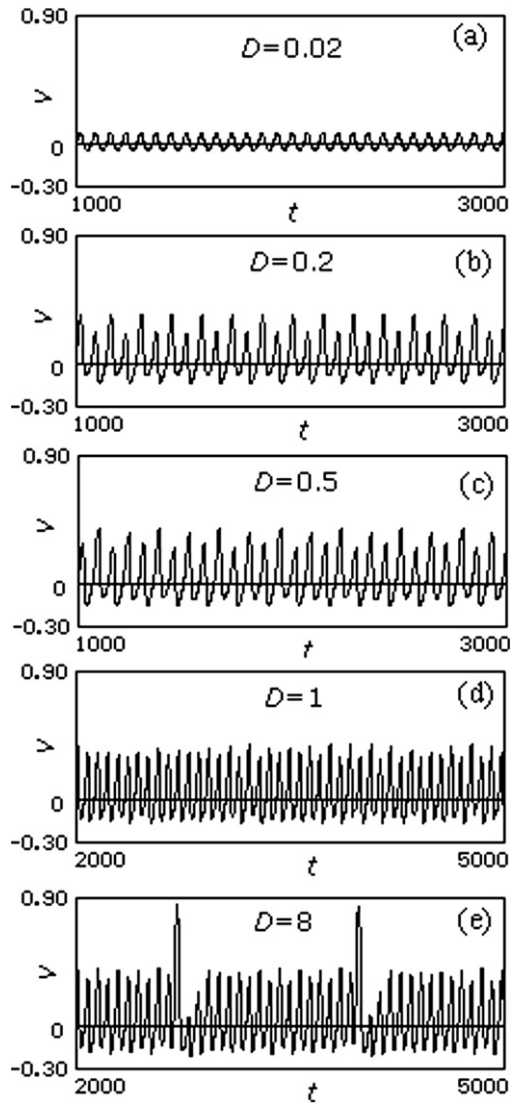

Fig. 2. Diffusion induced bifurcations at the interface x_0 ($x = 100$). (a) Simple, period-1 oscillations; (b) period-2; (c) period-4; (d) low amplitude chaotic; (e) intermittency.

of a uniform excitable medium. This was done by adding to the equation of $\frac{\partial v}{\partial t}$ the following term:

$$A_{\mathrm{ex}} \sum_{m=0}^{\infty} \delta(t - mT_{\mathrm{ex}}), \tag{2}$$

where A_{ex} is the amplitude of the external excitations, and δ is the Dirac delta function. The uniform medium had the same parameters as the right-hand region discussed above, and the amplitudes of the external excitations were chosen to be the same as those in Fig. 2(b), (c). Here, stable traveling pulses were observed only if the values of D were in the range $0.004 \leqslant D \leqslant 0.4$ (dimensionless units). The chosen values are considerably smaller than $D = 8$, because a localized excitation of limited spatial extent creates a stronger diffusion current (see below). This verified our assumption that different diffusion couplings can initiate, as well as suppress, the propagation of pulses in the excitable region.

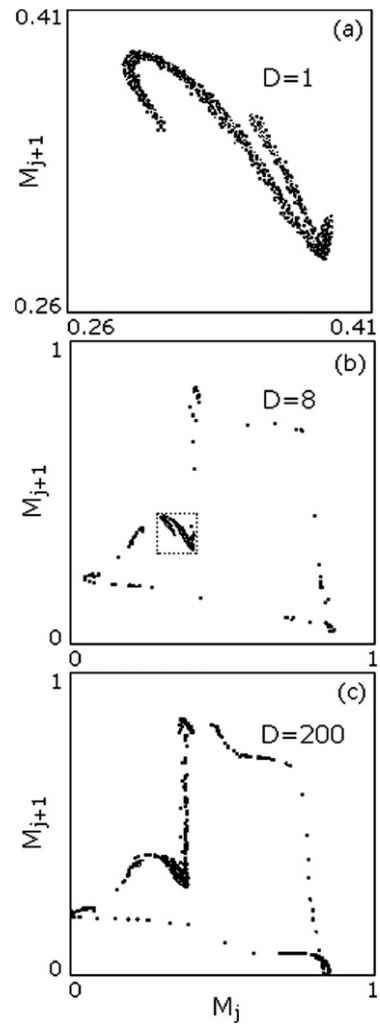

Fig. 3. First return maps for the chaotic oscillations at the interface x_0 ($x = 100$) shown in the preceding figure. They represent successive maxima of v: M_{j+1} vs. M_j.

Note that, from the viewpoint of nonlinear dynamics theory, the chaotic time evolution in Fig. 2(e) represents an example of intermittency which can arise after period doubling bifurcations, as a result of "switching" between different attractors [32,33,39]. Here a somewhat similar route to this type of intermittency is achieved by chaotic switching between the diffusion-induced strange (or periodic) attractor with low amplitudes, and the large-amplitude excitable spikes. Such coexistence of the diffusion induced oscillations, and the inherent excitable dynamics, may represent a new type of canards which combine excitable and oscillatory features [34]. But the usual, autonomous canards in a diffusionless FHN system are *two-dimensional*, and hence, can display intermittent chaos only in the presence of noise [35]. By contrast, the diffusion-induced "canards" are *three-dimensional* and therefore enable us to generate a completely deterministic intermittency.

3. The role of sizes of the adjacent regions

The influence of the SN and atrium sizes, and their mutual coupling, on the cardiac dynamics, was studied in the semi-

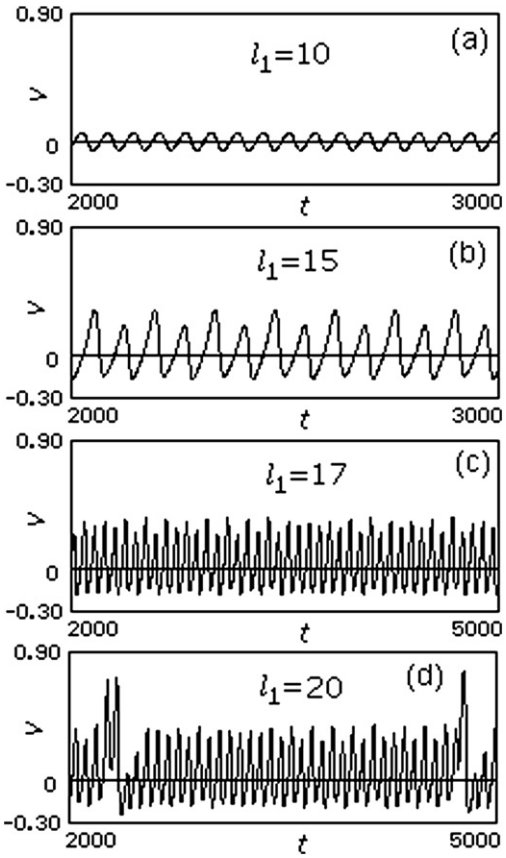

Fig. 4. Period-doubling route to chaos at the interface, generated by an increase in the size l_1 of the LC region. (a) Period-1 oscillations; (b) period-2; (c) low amplitude chaotic; (d) intermittency.

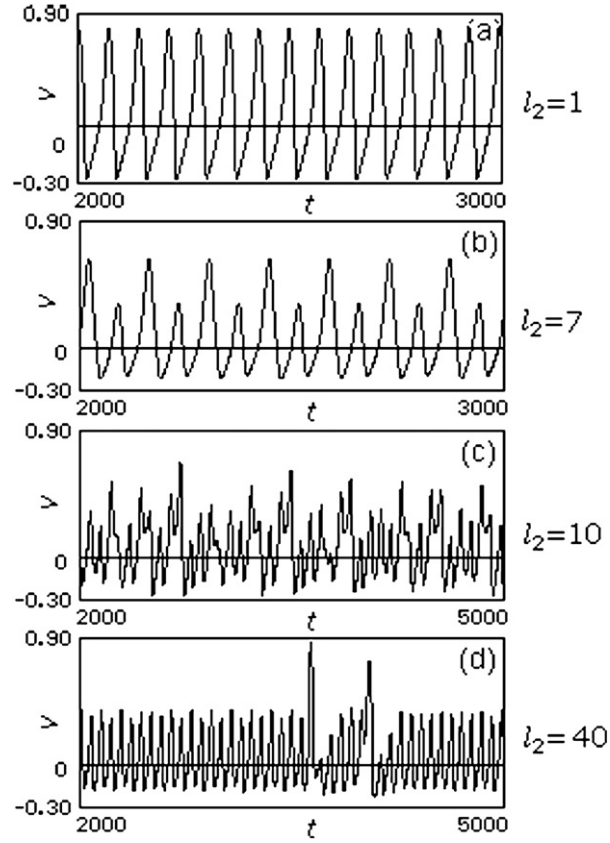

Fig. 5. Bifurcation transitions at the interface generated by an increase in the size l_2 of the excitable region. (a) Period-1 oscillations; (b) period-2; (c) low amplitude chaotic; (d) intermittency. Note that the amplitude of oscillations progressively decreases with the increasing complexity at the interface.

nal paper by Joiner and van Capelle [36]. In this section we follow [36], and check whether, in addition to changes in the diffusion coefficient, the *size* variation of the adjacent regions also leads to changes in the interface oscillations, and generates different wave trains. We investigate the interface dynamics as a function of l_1, the length of the LC region, under constant values of the diffusion coefficient ($D = 8$), and of l_2, the length of the excitable region. The results show that an increase of l_1 from its minimal value leads to the appearance of small periodic oscillations at the interface; these transform via period-doubling bifurcations, into chaotic oscillations with enlarged amplitudes, which, in turn, transform into large-amplitude intermittency (Fig. 4). This behavior is similar to the one previously obtained by increasing D, and can be explained in the following manner.

Keeping $l_2 = 100$ constant, let us first assume that the length of the left LC region is just $l_1 = 1$, i.e., one elementary interval at $x_0 - 1$, coupled by diffusion to that at x_0. The oscillation amplitude of this LC element at the interface will be lower that its natural one, due to the presence of a diffusion current towards the right. Next, *add* a second LC elementary interval at $x_0 - 2$, making $l_1 = 2$. This, in turn, will oscillate at a lower-than-natural amplitude, yet a bit higher than $x_0 - 1$ in the previous step. The element at $x_0 - 1$ will now oscillate at a higher amplitude than in the previous step, when it stood alone, because it now "receives" a diffusion current from the left, prior to "transmitting" it at the interface, into the right-hand excitable region. The result therefore is an *increase of the driving amplitude at the interface*. The described "thought" experiment can be carried on in building the transition zone further and further, until a certain limit size is obtained for the LC region, beyond which the process ceases to be "felt" at the interface.

Next, we changed the values of l_2, while keeping $l_1 = 100$ and $D = 8$ fixed. An increase of l_2 from its smallest value ($l_2 = 1$) resulted in a bifurcation evolution to more complex interface oscillations with progressively decreasing amplitudes (Fig. 5). The decrease in amplitudes, which is similar to that obtained in [36], occurs because the same diffusion current from the LC region spreads over a growing number of excitable points. This gradually decreasing current induces different sub-threshold oscillations in neighboring excitable points.

4. The influence of frequency oscillations in the LC region

By increasing the parameter d_1, more regular oscillations, with shorter time intervals between nearest spikes, are obtained at the interface. Consequently, the pulses in the right region also become more regular, and more frequent.

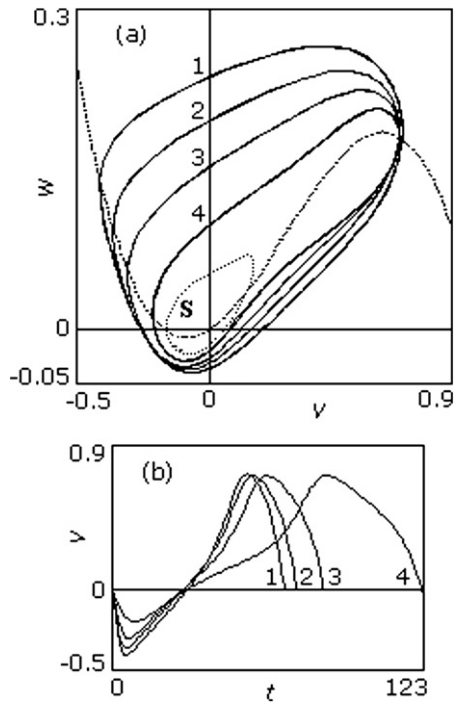

Fig. 6. Phase-space trajectories (a), and time evolutions (b) at the left region point x_1 ($x = 20$), for different values of d_1: (1) $d_1 = 1.5$; (2) $d_1 = 2$; (3) $d_1 = 2.5$; (4) $d_1 = 3$. The increase in d_1 results in shortening of the phase-space trajectories, and in creation of a closed *separatrix* curve S shown by the dotted line, $d_1 = 3$. The trajectories that come close to the separatrix display oscillations with ever increasing periods: $T(1) = 73$; $T(2) = 79$; $T(3) = 93$; $T(4) = 123$; ($\Delta t = 0.5$). Also shown is the v-nulcline, dash-dot.

In order to clarify these effects we first consider what happens in the driving LC region. For the present values of parameters, an increase in d_1 leads—at any point inside the LC region, but not too close to the interface (Fig. 6)—to a reduction of size of phase-space trajectories (Fig. 6(a)). The smaller limit cycles, however, exhibit an *increase* in the period of the local oscillations, together with an insignificant decrease in their amplitude (Fig. 6(b)). Similar phenomena, sometimes referred to as *negative* nonlinear dispersion [37], were observed in the FHN system in the vicinity of subcritical, as well as supercritical Hopf bifurcations [19,38]. Here the first type of bifurcation transition is present, when an increase in d_1 above some critical value, leads to the stabilization of the hitherto unstable focus $v = w = 0$. This is accompanied by the creation of a closed *separatrix* curve, between two concentric basins of attraction: an internal stable focus, and an external stable LC. The bifurcation value of d_1 may be analytically determined. By standard stability analysis of an uncoupled LC oscillator ($D = 0$), the eigenvalues of the linearized system near a stable focus must be complex conjugate with negative real parts [39]. The conditions for this are

$$4\varepsilon_1(a_1 d_1 + 1) - (\varepsilon_1 d_1 + a_1)^2 > 0 \quad \text{and} \quad (\varepsilon_1 d_1 + a_1) > 0. \tag{3}$$

The first condition is always satisfied while the second yields

$$d_1 > -a_1/\varepsilon_1, \tag{4}$$

giving $d_1 > 2.667$ for the present values of $a_1 = -0.16$ and $\varepsilon_1 = 0.06$. Numerical results show that a nonzero diffusion term noticeably lowers this bifurcation value giving, e.g., $d_1 > 2.57$ for $D = 8$. Now, the increase in the period of the LC oscillations, especially for larger d_1 values, is due to a slow motion in the vicinity of the above mentioned separatrix (unstable LC), resulting in generation of canard-like orbits [40], as shown in Fig. 6(a).

The stabilizing effect of such lengthy oscillations on the interface dynamics may be explained by a gradual approach of their frequencies to a "strong resonance" when every nth oscillation in the left region generates a large-amplitude spike at the interface.

5. Non-feedback chaos control

The above mentioned bistable oscillators, also called oscillators with "black holes", were discussed, e.g., in Ref. [41]. When coupled by diffusion, they exhibit properties either of a pure LC, or of an excitable medium. Depending on the initial excitations, they can sustain either collective "natural frequency" oscillations, or the propagation of a single pulse [42,43]. In a recent paper [19] it was shown that this feature allows an interesting effect, where a bistable oscillator can lock a *lower* frequency from an external periodic source. Such "abnormal" frequency-locking was studied in a simple system comprised of two uniform, spatially adjoining regions, of different types: a low frequency pure LC region and a bistable (LC/excitable) one. The same effect is used here to demonstrate the possibility of a simple non-feedback control of chaotic wave trains.

The existing non-feedback strategies for chaos control [44] typically utilize external periodic driving of *higher* frequency, and become inefficient in the case where frequency lowering is needed. Our approach, on the other hand, allows overcoming this inefficiency, at least for bistable chaotic systems. To show this we examine an extended medium composed of three uniform regions operating respectively, in pure LC, bistable (LC/excitable), and excitable modes (Fig. 7(a), (b)). The regions' parameters were selected in such way that the natural frequency in the left region was lower than that of the LC part of the middle one, thus allowing an abnormal frequency-locking. Moreover, the parameter $a_3 = 0.12$ in the right, excitable region here is higher than $a_2 = 0.015$ of the preceding sections. This permits generation of chaotic wave trains when the left region is absent, or when the locking of its (lower) frequency becomes impossible. The latter case occurs if strong initial excitation is applied at a sufficiently large part of the middle, bistable region. This region thereafter operates in the oscillatory regime, and its own higher-frequency oscillations induce intermittent chaos at the bistable/excitable interface (Fig. 7(c)), which in turn generates chaotic wave trains in the right region.

The situation is changed when an initial excitation is applied inside the left, pure LC region. Now the lower frequency of this region is locked by the middle one, which operates in the excitable mode. The ensuing slower periodic motion of the middle region induces regular oscillations in a bistable/excitable interface (Fig. 7(d), (e)). The chaotic wave trains can thus be

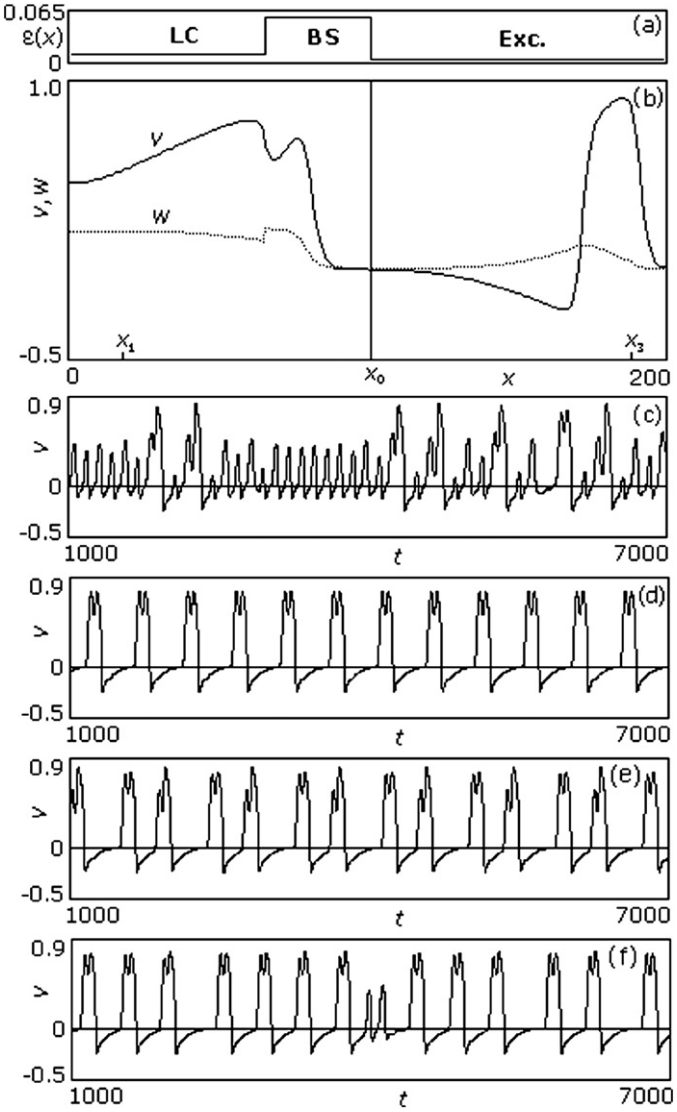

Fig. 7. Low-frequency control of chaotic wave trains. (a) The $\varepsilon(x)$ profile in the three regions: $a_1 = -0.16$, $\varepsilon_1 = 0.01$ for $0 \leqslant x < 70$ (LC); $a_2 = -0.16$, $\varepsilon_2 = 0.056$ for $70 \leqslant x < 100$ (BS, bistable), and $a_3 = 0.12$, $\varepsilon_3 = 0.005$ for $100 \leqslant x \leqslant 200$ (excitable); $d = 3$, and $D = 1$ throughout; (b) v and w space profiles in the heterogeneous medium; stimulation in the LC region. (c) Strongly chaotic oscillations at the interface, $x_0 = 100$, arising when the initial stimulation is launched throughout the BS region. (d) The interface oscillations become periodic when the initial stimulation is launched anywhere in the LC region. (e) Same as (d), except for a smaller value of ε_1 ($\varepsilon_1 = 0.008$); here the simple, period-1, interface oscillations become complex, period-2. (f) Same as (d), except for a larger value of ε_1 ($\varepsilon_1 = 0.0124$); in this case the periodic interface oscillations become nearly periodic, i.e., slightly chaotic.

controlled, and transformed into periodic (Figs. 7(d), (e)), or nearly periodic (Fig. 7(f)) sequences of traveling pulses.

6. Discussion

The dynamical nature of fibrillations in the mammalian heart is not fully understood, but is believed to be the result of 2D spiral, or 3D scroll wave propagation, and their breakup into many small, asynchronous wavelets [45,46]. In this Letter we demonstrate that even in a one-dimensional model, an alternative fibrillation mechanism, may arise as a result of chaotic motion at the interface between clusters of self-oscillating cardiac cells, and the surrounding excitable tissue. In addition to the SN/myocardium, such interfaces are also found at the boundaries of the atrioventricular node, the Purkinje fibers, as well as pathological *ectopic* sources. For example, the chaotic wave trains discussed in Sections 2, 5 may be associated with *SN-induced* paroxysmal atrial fibrillations (see [47,48], and references therein).

In a previous paper we have utilized bistable oscillators to portray the complex heterogeneous structure of the cardiac SN [19]. The SN center there was simulated by a low-frequency, pure LC region, while the peripheral zone, the *perinode*, was assumed to operate as a bistable regime. Due to the abnormal frequency-locking, the low frequency center operates as the driver of the entire heart. The results obtained in Section 5 here, regarding the "switching" between strongly chaotic, and nearly periodic wave trains, reveal new properties of this model. As was shown, external interventions, as well as an anomalous intercellular coupling, can shift the leading site from the SN center to its perinode [49,50]. From our simulations it follows that such a shift can result in the generation of strongly chaotic wave trains (Fig. 7(c)) associated with AF. This, in turn, could be stabilized by restoring the leading site to its normal location (Figs. 7(d)–(f)).

References

[1] L. Glass, M.C. Mackey, From Clocks to Chaos: The Rhythms of Life, Princeton Univ. Press, Princeton, NJ, 1988.
[2] A.V. Panfilov, A.V. Holden, Computational Biology of the Heart, Wiley, New York, 1997.
[3] A. Garfinkel, M.L. Spano, W.L. Ditto, J.N. Weiss, Science 257 (1992) 1230.
[4] D.J. Christini, J.J. Collins, Phys. Rev. E 53 (1996) R49.
[5] W.L. Ditto, et al., Int. J. Bifur. Chaos 10 (2000) 593.
[6] H.N. Pak, et al., J Cardiovasc. Electrophysiol. 15 (2004) 581; Z. Qu, Electrophysiology 15 (2004) 1186.
[7] C. Poon, C. Merrill, Nature 389 (1997) 492.
[8] S. Schiff, et al., Nature 370 (1994) 615.
[9] X. Wang, G. Chen, X. Yu, Chaos 10 (2000) 771.
[10] M. Feingold, et al., Phys. Rev. A 37 (1988) 4060.
[11] A. Rabinovitch, R. Thieberger, M. Friedman, Phys. Rev. E 50 (1994) 1572.
[12] D.T. Kaplan, et al., Phys. Rev. Lett. 76 (1996) 4074.
[13] S. Coombes, A.H. Osbaldestin, Phys. Rev. E 62 (2000) 4057.
[14] Y. Horikawa, Phys. Rev. E 50 (1994) 1708; Y. Horikawa, Biol. Cybern. 79 (1998) 251.
[15] V. Votrubovà, et al., J. Phys. Chem. A 102 (1998) 1318.
[16] I. Schreiber, P. Hasal, M. Marek, Chaos 9 (1999) 43.
[17] T.S. Achromeeva, et al., Phys. Rep. 176 (1989) 189.
[18] V. Rai, G. Jayaraman, Curr. Sci. India 84 (2003) 925.
[19] M. Gutman, I. Aviram, A. Rabinovitch, Phys. Rev. E 70 (2004) 037202.
[20] M. Gutman, I. Aviram, A. Rabinovitch, Phys. Rev. E 69 (2004) 016211.
[21] A. Rabinovitch, M. Gutman, I. Aviram, J. Biol. Phys. 28 (2002) 713.
[22] R. FitzHugh, Biophys. J. 1 (1961) 445.
[23] A. Rabinovitch, et al., J. Theor. Biol. 196 (1999) 141.
[24] M. Friedman, A. Kandel, Fundamentals of Computer Numerical Analysis, CRC Press, Boca Raton, FL, 1994.
[25] Y. Kuramoto, Chemical Oscillations, Waves and Turbulence, Springer, Berlin, 1984.
[26] P. Ortoleva, J. Ross, J. Chem. Phys. 58 (1973) 5673.
[27] M.C. Cross, P.C. Hohenberg, Rev. Mod. Phys. 65 (1993) 892.
[28] R. Faller, L. Kramer, Phys. Rev. E 57 (1998) R6249.

[29] L. Brusch, Phys. Rev. Lett. 85 (2000) 86.
[30] H.A. Fozzard, M. Schoenberg, J. Physiol. (London) 226 (1972) 593.
[31] J.C. Neu, R.S. Preissig Jr., W. Krassowska, Physica D 102 (1997) 285.
[32] Da-Ren He, et al., Phys. Lett. A 171 (1992) 61.
[33] V. Gontar, M. Gutman, Math. Comput. Mod. Dynamical Systems 5 (1999) 203.
[34] H.G. Rotstein, N. Kopell, A.M. Zhabotinsky, I.R. Epstein, SIAM J. Appl. Math. 63 (2003) 1998.
[35] F. Marino, et al., Phys. Rev. Lett. 92 (2004) 073901.
[36] R.W. Joyner, F.J.L. van Capelle, Biophys. J. 50 (1986) 1157.
[37] J.A. Sepulchre, G. Dewel, A. Babloyantz, Phys. Lett. A 147 (1990) 380.
[38] A. Rabinovitch, M. Gutman, I. Aviram, Phys. Rev. E 67 (2003) 036212.
[39] S.H. Strogatz, Nonlinear Dynamics and Chaos: With Applications to Physics, Biology, Chemistry and Engineering, Addison–Wesley, Reading, MA, 1994.
[40] M. Argentina, P. Coullet, V. Krinsky, J. Theor. Biol. 205 (2000) 47.
[41] J.D. Murray, Mathematical Biology, second corrected ed., Springer-Verlag, Berlin, 1993.
[42] R. Kobayashi, T. Ohta, Y. Hayase, Phys. Rev. E 50 (1994) R3291.
[43] B. Ermentrout, X. Chen, Z. Chen, Physica D 108 (1997) 147.
[44] S. Boccaletti, et al., Phys. Rep. 329 (2000) 103.
[45] R.A. Gray, A.M. Pertsov, J. Jalife, Nature 392 (1998) 75.
[46] A. Karma, Chaos 4 (1994) 461.
[47] J.E. Olgin, D.P. Zipes, in: E. Braunwald, D.P. Zipes, P. Libby (Eds.), Heart Disease, sixth ed., Saunders, Philadelphia, 2001, p. 815.
[48] P. Östborn, B. Wohlfart, G. Ohlén, J. Theor. Biol. 211 (2001) 201; P. Östborn, B. Wohlfart, G. Ohlén, J. Theor. Biol. 211 (2001) 219.
[49] T. Opthof, Cardiovasc. Drugs Therapy 1 (1988) 573.
[50] A. Garny, et al., J. Cardiovasc. Electrophysiol. 14 (2003) S121.